Biochemical and Electrochemical Characterization of Quinohemoprotein Amine Dehydrogenase from *Paracoccus denitrificans*†

Kazuyoshi Takagi, Masaki Torimura, Katsunori Kawaguchi, Kenji Kano,* and Tokuji Ikeda

Division of Applied Life Sciences, Graduate School of Agriculture, Kyoto University, Sakyo-ku, Kyoto 606-8502, Japan

Received December 1, 1998; Revised Manuscript Received March 1, 1999

ABSTRACT: A new quinohemoprotein amine dehydrogenase from *Paracoccus denitrificans* IFO 12442 was isolated and characterized in views of biochemistry and electrochemistry. This enzyme exists in periplasm and catalyzes the oxidative deamination of primary aliphatic and aromatic amines. *n*-Butylamine or benzylamine as a carbon and energy source strongly induces the expression of the enzyme. Carbonyl reagents inhibit the enzyme activity irreversibly. This enzyme is a heterodimer constituted of α and β subunits with the molecular mass of 59.5 and 36.5 kDa, respectively. UV−vis and EPR spectroscopy, and the quinone-dependent redox cycling and heme-dependent peroxidative stains of SDS−PAGE bands revealed that the α subunit contains one quinonoid cofactor and one heme *c* per molecule, while the β subunit has no prosthetic group. The redox potential of the heme *c* moiety was determined to be 0.192 V vs NHE at pH 7.0 by a mediator-assisted continuous-flow column electrolytic spectroelectrochemical technique. The analysis of the substrate titration curve allowed the evaluation of the redox potential of the quinone/semiquinone and semiquinone/quinol redox couples as 0.19 and 0.11 V, respectively.

Since the first report on bacterial amine oxidation by Eady and Large (*1*), several types of amine dehydrogenases have been purified and characterized. Methylamine dehydrogenase (MADH)[1] (*1*−*6*) and aromatic amine dehydrogenase (AADH) (*7*, *8*) have been most extensively studied among them. The two enzymes have $\alpha_2\beta_2$ structures and contain a covalently bound organic cofactor in each of the β subunits, while the larger α subunit does not possess any prosthetic group. There is no redox-active metal ion in the enzymes. The enzymes have a unique organic cofactor:tryptophan tryptophylquinone (TTQ) (*9*). After the discovery of TTQ, a model compound of TTQ was synthesized and the chemistry of the model compound was examined in view of model reactions of amine dehydrogenases (*10*−*14*).

On the other hand, quinohemoprotein amine dehydrogenase (AMDH) has been isolated from *Pseudomonas putida* (*15*−*18*). AMDH was at first reported as an enzyme composed of two subunits with 60 and 40 kDa in the molecular mass (*15*, *17*). The 60 kDa subunit contains two heme *c* moieties (*16*) and a quinonoid cofactor (*17*). Recent report, however, revealed the presence of an additional 20 kDa subunit, in which the quinonoid cofactor is localized (*18*). Detailed thermodynamic and kinetic properties of this enzyme remain to be elucidated.

Here we describe the purification and characterization of a new quinohemoprotein amine dehydrogenase (QH-AmDH) from *Paracoccus denitrificans* IFO 12442, grown with methylamine, *n*-butylamine, or benzylamine as a major source of carbon and energy. The subunit structure and spectroscopic properties were characterized by conventional methods and the redox potential of the heme moiety was determined by a mediator-assisted continuous-flow column electrolytic spectroelectrochemical technique developed in our laboratory (*19*). The substrate titration curve was also analyzed to assess the redox potential of the quinonoid cofactor. On the basis of the above results, the electron-transfer reaction catalyzed by this enzyme is discussed from the physiological points of view.

EXPERIMENTAL PROCEDURES

Bacterial Growth. P. denitrificans IFO 12442 was purchased from the Institute for Fermentation in Osaka (Japan) and was grown aerobically at 30 °C in the medium containing 1% K_2HPO_4, 0.5% KH_2PO_4, 0.05% $MgSO_4 \cdot 7H_2O$, 0.05% yeast extract, and 0.5% amine hydrochloride (methylamine, *n*-butylamine, or benzylamine) as a carbon source. The pH of the medium was adjusted to 7.0. For the purification of amine dehydrogenases, the cells were grown with methylamine in a 50 L fermenter for 24 h and harvested by centrifugation.

† This work was supported in part by a Grant-in-Aids for Scientific Research from the Ministry of Education, Science, Sports, and Culture of Japan.

* To whom correspondence should be addressed. Phone: +81-75-753-6393. Fax: +81-75-753-6128. E-mail: kkano@kais.kyoto-u.ac.jp.

[1] Abbreviations: MADH, TTQ-containing methylamine dehydrogenase; TTQ, tryptophan tryptophylquinone; AADH, TTQ-containing aromatic amine dehydrogenase; AMDH, quinohemoprotein amine dehydrogenase from *Pseudomonas putida*; QH-AmDH, quinohemoprotein amine dehydrogenase from *Paracoccus denitrificans* IFO 12442; DCIP, 2,6-dichloroindophenol; PES, phenazine ethosulfate; DMBQ, 2,6-dimethyl-1,4-benzoquinone; NHE, normal hydrogen electrode; k_{cat}, catalytic constant; K_m(S), Michaelis constant for substrate; K_m(A), Michaelis constant for electron acceptor; ϵ, absorption coefficient; A_λ, absorbance at the wavelength λ; *E*, electrode potential or equilibrated solution potential; $E_H^{\circ\prime}$, redox potential of the heme *c* moiety; $E_{Q1}^{\circ\prime}$, redox potential of the quinone/semiquinone couple; $E_{Q2}^{\circ\prime}$, redox potential of the semiquinone/quinol couple; *F*, Faraday constant; *R*, gas constant; *T*, absolute temperature; K_{sem}, semiquinone formation constant; PQQ, pyrroloquinoline quinone.

10.1021/bi9828268 CCC: $18.00
Published on Web 05/06/1999

Purification of Amine Dehydrogenases. All purification procedures were performed at 4 °C. About 100 g of freshly harvested cells was suspended in 500 mL of 10 mM potassium phosphate, pH 7.5 (buffer A), and then disrupted by ultrasonic disintegration. The resulting lysate was centrifuged at 40000*g* for 60 min, and the supernatant solution was dialyzed overnight against 5 L × 2 of buffer A. The dialyzed solution was applied to a DEAE-cellulose column (200 mL) equilibrated with buffer A. The column was eluted with a linear gradient of 0−0.5 M NaCl in the same buffer (2 L). Two kinds of spectrophotometric assay of amine dehydrogenase activity were separately performed for each fraction using methylamine (0.1 mM) as a substrate; one is the reduction of $Fe(CN)_6^{3-}$ (1 mM) (methylamine-dependent $Fe(CN)_6^{3-}$-reducing activity) and the other is the reduction of 2,6-dichloroindophenol (DCIP) (50 μM) in the presence of 3 mM phenazine ethosulfate (PES) as an electron-transfer mediator (methylamine/PES-dependent DCIP-reducing activity). In the following, the MADH and QH-AmDH fractions were separately treated with identical procedures. Solid $(NH_4)_2SO_4$ was added to the enzyme fractions as 1.5 M and the enzyme solution was applied to a Butyl-Toyopearl column (100 mL) equilibrated with 1.5 M $(NH_4)_2SO_4$ in 0.1 M potassium phosphate, pH 7.5 (buffer B). After being washed with the $(NH_4)_2SO_4$-containing buffer B, the column was eluted with a linear gradient (500 mL) of 1.5 to 0 M $(NH_4)_2SO_4$ in buffer B. Finally, the enzyme was purified by a Q-Sepharose column (50 mL), eluted with a linear gradient (500 mL) of 0.2−0.4 M NaCl in buffer A. The enzyme thus purified to homogeneity was concentrated, dialyzed against buffer A, and stored frozen for future use.

Preparation of Periplasmic Fraction. The method is based on that first reported by Alefounder and Ferguson (*20*) and practically identical with that used in the first step of the purification of MADH from *P. denitrificans* ATCC 13543 (*6*, *21*). Cells were suspended in 20 mL/g wet weight of cells of 20 mM potassium phosphate (pH 7.5) containing 0.5 M sucrose and 0.5 mM EDTA. Lysozyme (5 mg/g wet weight of cells), dissolved in water to 10 mg/mL, was added to the cell suspension and followed by equal volume of water. After incubation at 30 °C for 20 min under gentle swirling, the suspension was centrifuged at 20000*g* for 20 min to remove spheroplasts and unbroken cells (if any) from the periplasmic fraction.

Electrophoresis and Gel Chromatography. Polyacrylamide gel electrophoresis in the absence [native-PAGE (*22*)] and presence of sodium dodecyl sulfate [SDS−PAGE under reducing conditions (*23*)] were performed according to the literature. The gels were stained with CBB R-250 to detect protein fractions. The SDS−PAGE gels were also subjected separately to the quinone-dependent redox-cycling stain (*24*) and the heme-dependent peroxidative stain (*25*) for the detection of quinonoid cofactor and heme, respectively. High-performance gel filtration chromatography was carried out with a Superdex 200 HR 10/30 column.

Analysis of Heme c Content. The total number of heme units was evaluated from difference spectra between $S_2O_4^{2-}$-reduced and $Fe(CN)_6^{3-}$-oxidized forms of pyridine hemochrome, which was prepared by mixing the sample with a final concentration of 20% (v/v) pyridine and 50 mM NaOH. The heme content was calculated using the absorbance coefficient of 30.3 mM^{-1} cm^{-1} at 550 nm (*26*). Protein concentrations were determined by a modified Lowry method (*27*) with bovine serum albumin as a standard or by weighing deionized and lyophilized samples. Deoinization was performed by dialysis against water (five times).

Spectroscopy. UV−vis absorption spectra were recorded with Shimadzu UV-2500(PC)S or Shimadzu UV-260 spectrophotometers. Before spectroscopic measurements of QH-AmDH, the enzyme was completely oxidized with $K_3Fe(CN)_6$ and then removed it by dialysis. EPR spectra were recorded on a Nikkiso ES-10 spectrometer with a glass capillary cell with an inner diameter of 0.7 mm. The magnitude of the modulation (100 kHz) was chosen to be as low as possible to optimize the resolution and signal-to-noise ratio of observed spectra. The microwave power was set to 1−2 mW. All EPR spectral measurements were performed at room temperature.

Titrations. Anaerobic reductive titration of QH-AmDH were performed with *n*-butylamine or sodium dithionite as reductant at room temperature in 0.1 M potassium phosphate buffer (pH 7.5) in a nitrogen gas-purged drybox. Moistured argon gas was passed through the enzyme and reagent solutions to remove dissolved dioxygen. Aerobic titration of QH-AmDH with *p*-nitrophenylhydrazine hydrochloride or phenylhydrazine hydrochloride was also carried out at room temperature in the same buffer (pH 7.5).

Enzyme Assay. Steady-state kinetic assays for QH-AmDH activity were performed spectrophotometrically by measuring the amine-dependent reduction rate of $Fe(CN)_6^{3-}$ at 417 nm and at 25 °C. The reaction mixture contained appropriate amounts of $K_3Fe(CN)_6$ and substrate amine in 0.1 M potassium phosphate (pH 7.5). The reactions were initiated by addition of an aliquot of enzyme solutions. In measurements of the electron acceptor specificity, $K_3Fe(CN)_6$ was replaced by DCIP or PES coupled with DCIP. To determine steady-state kinetic parameters, initial rates were measured at several concentrations of substrates or electron acceptors.

Mediator-Assisted Continuous-Flow Column Electrolytic Spectroelectrochemistry. This technique is based on the spectroscopic detection of the redox states of proteins equilibrated in a continuous-flow redox buffer regulated by column electrolysis (*19*). In the present study, a portion of a protein sample (10 μL × ca. 57 μM) was injected on a mobile phase buffer (pH 7.0) and mixed with a mediator solution on a two-channel flow injection system. 2,6-Dimethyl-1,4-benzoquinone (DMBQ; $E^{\circ\prime} = 0.175$ V at pH 7.0) was used as a mediator at a final concentration of 1.0 mM. The mediator solution and a mobile phase buffer were thoroughly deaerated with nitrogen gas and flowed at 0.5 mL min^{-1}, unless otherwise stated. Other details of the principle, instruments, and methods are described in the literature (*19*). All the potentials in this paper are referred to the normal hydrogen electrode (NHE).

RESULTS

Purification of QH-AmDH. The cell-free extract of *P. denitrificans* IFO 12442 grown with methylamine as a carbon source afforded one peak with the methylamine/PES-dependent DCIP-reducing activity at ca. 0.2 M NaCl region in the DEAE-cellulose column NaCl-gradient chromatographic separation (Figure 1, curve C). The succeeding chromatographic purification from the fraction revealed that

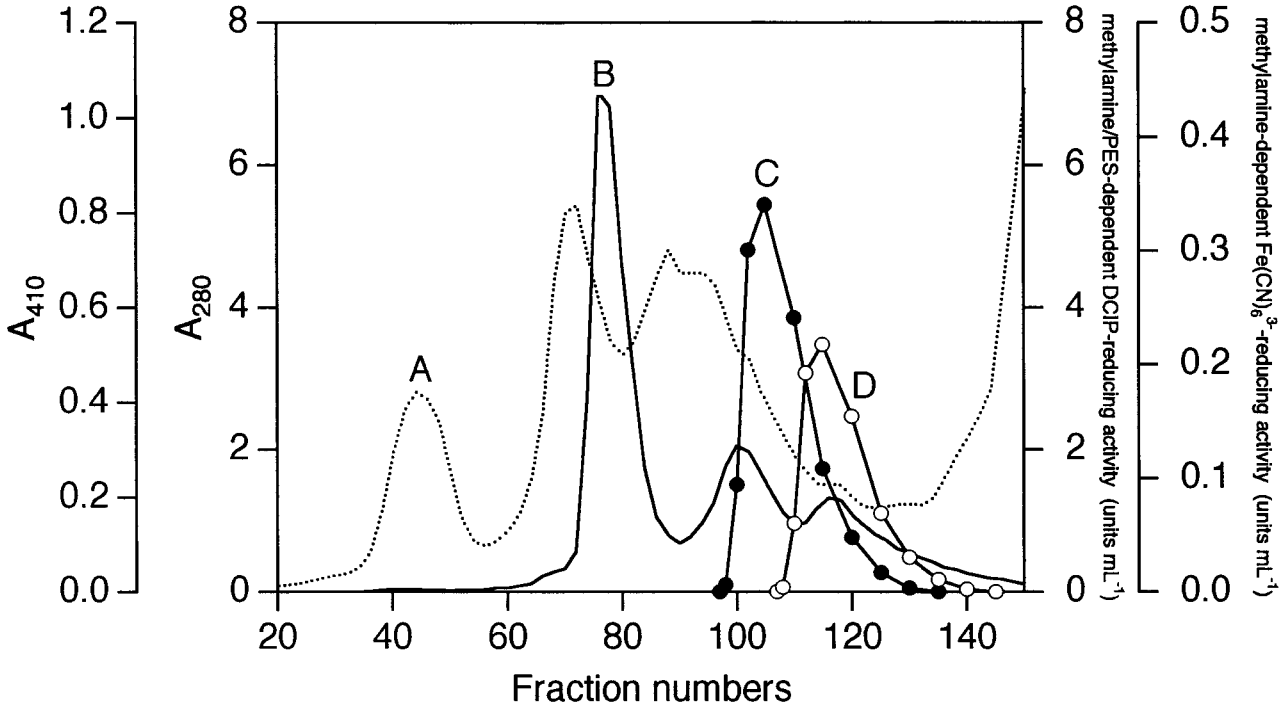

FIGURE 1: Elution profile of amine dehydrogenases in DEAE-cellulose column chromatography. Each fraction was collected with a volume of 11.5 mL. Absorption measurements at 280 (A) and 410 nm (B) reflect the elution of protein and heme *c* proteins, respectively. Methylamine/PES-dependent DCIP-reducing activity (C) and methylamine-dependent $Fe(CN)_6^{3-}$ -reducing activity (D) were measured as described in the text.

the predominant enzyme is identical with TTQ-containing MADH produced by *P. denitrificans* ATCC 13543 (*6*, *28*). The chromatographic separation gave three peaks of hemoproteins (Figure 1, curve B). While amine dehydrogenase activity was not detectable in the fractions of the first and second peaks, the third peak overlapping with the MADH peak contained *c*-type cytochrome exhibiting the strong methylamine-dependent $Fe(CN)_6^{3-}$ -reducing activity (Figure 1, curve D). The succeeding chromatographic purification of the heme *c* containing amine dehydrogenase resulted in a single band on native-PAGE and a single symmetrical peak on high-performance gel chromatography. The yield of heme *c* containing amine dehydrogenase was 12 mg from 100 g of freshly harvested cells by the procedure described above.

The molecular mass of the heme *c*-containing amine dehydrogenase was assessed to be ca. 100 kDa by high-performance gel chromatography. The enzyme gave two distinct bands in SDS−PAGE, which corresponded to 59.5 kDa (α subunit) and 36.5 kDa (*β* subunit) in the molecular mass (Figure 2). The α subunit band was positive in both of the quinone-dependent redox-cycling stain and the heme-dependent peroxidative stain, while the *β* subunit band was negative. These data indicate that this enzyme is an *αβ* heterodimer quinohemoprotein amine dehydrogenase (QH-AmDH) with a molecular mass of 96 kDa and that the α subunit contains quinonoid cofactor and heme *c* moiety.

Steady-State Kinetics and Inhibition of QH-AmDH. Steady-state reaction velocity (*v*) of QH-AmDH followed the Michaelis−Menten equation for both methylamine and $Fe(CN)_6^{3-}$. Double reciprocal plots of *v* vs the methylamine concentration at several concentrations of $K_3Fe(CN)_6$ yielded a set of parallel lines. This supports a ping-pong mechanism for the enzymatic reaction. The catalytic constant (k_{cat}) and the Michaelis constant for substrate [K_m(S)] were determined

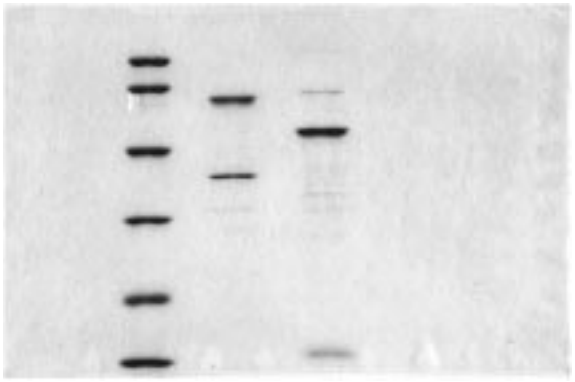

FIGURE 2: SDS−PAGE of QH-AmDH (center lane) and MADH (right lane) from *P. denitrificans* IFO 12442. The left lane contains molecular mass markers: phosphorylase *b* (97.4 kDa), bovine serum albumin (66.3 kDa), aldolase (42.4 kDa), carbonic anhydrase (30.0 kDa), soybean trypsin inhibitor (20.1 kDa), lysozyme (14.4 kDa).

for several aliphatic and aromatic amines using $Fe(CN)_6^{3-}$ as an electron acceptor. The results are summarized in Table 1. QH-AmDH exhibited relatively broad substrate specificity for primary aliphatic and aromatic amines, while it did not work on secondary and tertiary amines. QH-AmDH seems to prefer longer chain primary aliphatic amines to shorter chain amines. The Michaelis constants for some artificial electron acceptors [K_m(A)] as well as k_{cat} were also evaluated using methylamine as a substrate. The result is listed in Table 1. $Fe(CN)_6^{3-}$ works as an electron acceptor for QH-AmDH, though PES is a better one. This is in marked contrast with TTQ-containing MADH, of which K_m(A) for $Fe(CN)_6^{3-}$ was 4.5 mM with methylamine as a substrate.

Carbonyl reagents (hydrazine, hydroxylamine, phenylhydrazine, and semicarbazide) showed remarkable and irreversible inhibitory effects against the QH-AmDH activity. The

Table 1: Steady-State Kinetic Parameters of QH-AmDH

substrates	k_{cat} (s^{-1})	K_m(S) (μM)[a]	k_{cat}/K_m(S) (M^{-1} s^{-1})
methylamine	14	1.3×10^3	1.1×10^4
ethylamine	13	1.0×10^2	1.3×10^5
propylamine	27	<1.0	$>2.7 \times 10^7$
butylamine	22	<1.0	$>2.2 \times 10^7$
benzylamine	22	<1.0	$>2.2 \times 10^7$
phenethylamine	26	<1.0	$>2.6 \times 10^7$
electron acceptors	k_{cat} (s^{-1})	K_m(A) (μM)[b]	k_{cat}/K_m(A) (M^{-1} s^{-1})
$K_3Fe(CN)_6$	15	7.8×10^2	1.9×10^4
PES (+DCIP)[c]	7.1	1.4×10	5.1×10^5
DCIP	1.5	1.2×10^2	1.3×10^4

[a] $K_3Fe(CN)_6$ (1.0 mM) was used as an electron acceptor. [b] Methylamine (10 mM) was used as a substrate. [c] The DCIP concentration was fixed at 50 μM.

Table 2: Amine Dehydrogenase Activities in the Periplasmic Fraction of *P. denitrificans* Grown with Several Amines as Carbon Source

carbon source in growth	QH-AmDH activity (units/g wet cell)[a]	MADH activity (units/g wet cell)[b]
methylamine	0.12 (0.20)[c]	3.10 (5.41)[c]
butylamine	1.04 (1.55)[c]	~0 (~0)[c]
benzylamine	0.45 (0.77)[c]	~0 (~0)[c]

[a] *n*-Butylamine-dependent $Fe(CN)_6^{3-}$ -reducing activity. 1 unit = 2 μmol of $Fe(CN)_6^{3-}$ reduction/min. The reaction mixture contained 1 mM $K_3Fe(CN)_6$ and 0.1 mM *n*-butylamine in 0.1 M potassium phosphate (pH 7.5). [b] Methylamine/PES-dependent DCIP-reducing activity. 1 unit = 1 μmol of DCIP reduction/min. The reaction mixture contained 50 μM DCIP, 3 mM PES, and 0.1 mM methylamine in 0.1 M potassium phosphate (pH 7.5). [c] Total activity of cell extract.

inhibition is reasonably explained in terms of the Schiff base complex formation of the quinonoid cofactor in QH-AmDH with the carbonyl reagents. EDTA showed no detectable effects on the enzyme activity.

Expression and Location of Amine Dehydrogenases. Under the conditions of [*n*-butylamine] = 0.1 mM and [$Fe(CN)_6^{3-}$] = 0.1 mM, the apparent catalytic constants ($k_{cat,app}$) were 13 s^{-1} for QH-AmDH and 0.13 s^{-1} for MADH. Therefore, the *n*-butylamine-dependent $Fe(CN)_6^{3-}$ -reducing activity can be considered to represent the QH-AmDH activity. On the other hand, $k_{cat,app}$ under the conditions of [methylamine] = 0.1 mM, [PES] = 3 mM, and [DCIP] = 50 μM were 0.52 s^{-1} for QH-AmDH and 25 s^{-1} for MADH. Thus, the methylamine/PES-dependent DCIP-reducing activity can reflect the MADH activity. Table 2 shows the *n*-butylamine-dependent $Fe(CN)_6^{3-}$ -reducing activity (QH-AmDH activity) and methylamine/PES-dependent DCIP-reducing activity (MADH activity) in the periplasmic fraction and the total cell-free extract of *P. denitrificans* grown with methylamine, *n*-butylamine, or benzylamine as a source of carbon. The expression of the QH-AmDH activity is strongly induced by *n*-butylamine or benzylamine. The increased expression of QH-AmDH is reasonably understood in terms of the steady-state kinetic parameters given in Table 1. *n*-Butylamine and benzylamine are better substrates of QH-AmDH than methylamine. On the other hand, the MADH activity was not detectable in *P. denitrificans* grown with *n*-butylamine or benzylamine, indicating that methylamine is essential to express MADH. This also seems to be reasonable, because MADH shows relatively strong substrate specificity toward methylamine [K_m(S) = 20 μM and k_{cat} = 32 s^{-1} with PES/DCIP as electron acceptor (*29*)] and hardly works on benzylamine (*6*). *n*-Butylamine also is not a good substrate for MADH at least decreased concentrations [K_m(S) = 4.5 mM with PES/DCIP as electron acceptor (*29*)].

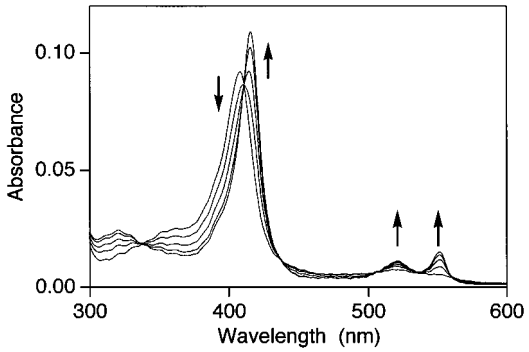

FIGURE 3: UV−vis absorption spectra of purified QH-AmDH. QH-AmDH (1.23 nmol in 3.0 mL) in 0.1 M potassium phosphate (pH 7.5) was titrated with *n*-butylamine. The spectra were recorded ca. 20 min after addition of 0, 0.4, 0.8, 1.2, and 2.0 nmol of *n*-butylamine under anaerobic conditions. The arrows indicate the direction of the spectral changes on the addition of *n*-butylamine.

The QH-AmDH activity and MADH activity in the periplasmic fraction of *P. denitrificans* grown with methylamine were 60 and 57% of the total activity of the cell extract, respectively, under our experimental conditions (Table 2). The relative activity of QH-AmDH in the periplasmic fraction was also evaluated as 67 and 61% for *P. denitrificans* grown with *n*-butylamine and benzylamine, respectively. Considering that MADH is a periplasmic enzyme (*30*), it can be safely concluded that QH-AmDH locates in the periplasm.

Spectral Properties. UV−vis spectra of QH-AmDH have revealed the presence of a typical *c*-type cytochrome (Figure 3). The fully oxidized form with $K_3Fe(CN)_6$ gave a Soret peak at 408 nm with an absorption coefficient (ϵ) of 227 mM^{-1} cm^{-1}. Addition of substoichiometric amounts of *n*-butylamine to QH-AmDH caused a decrease in the absorbance at 408 nm (A_{408}) and an increase in A_{416}, A_{522}, and A_{552}. Isosbestic points were observed at 341, 412, 439, 508, 537, and 560 nm. The fully reduced form gave three peaks at 416 (ϵ = 270 mM^{-1} cm^{-1}), 522 (ϵ = 27.8 mM^{-1} cm^{-1}), and 552 nm (ϵ = 37.2 mM^{-1} cm^{-1}) and was slowly reoxidized under aerobic conditions with a half-life time of ca. 23 min. The identical spectrum of the reduced QH-AmDH was obtained by the reduction with sodium dithionite. During the anaerobic reductive titration with substrate amine or dithionite, no clear spectral change due to the redox of the quinonoid cofactor was recognized. This would be ascribed to small absorption coefficient of the quinonoid cofactor compared with heme *c*.

The number of the heme group was evaluated to be 1.07/molecule based on the pyridine hemochrome method and the modified Lowry method. The protein concentration was also evaluated by a dry weight determination after the thorough removal of salts by dialysis and lyophilization. The dry weight method gave a value only 7% larger than that determined by the Lowry method. Then it can be concluded that QH-AmDH has 1 mol of *c*-type cytochrome/enzyme in the α subunit. This is supported by the occurrence of the

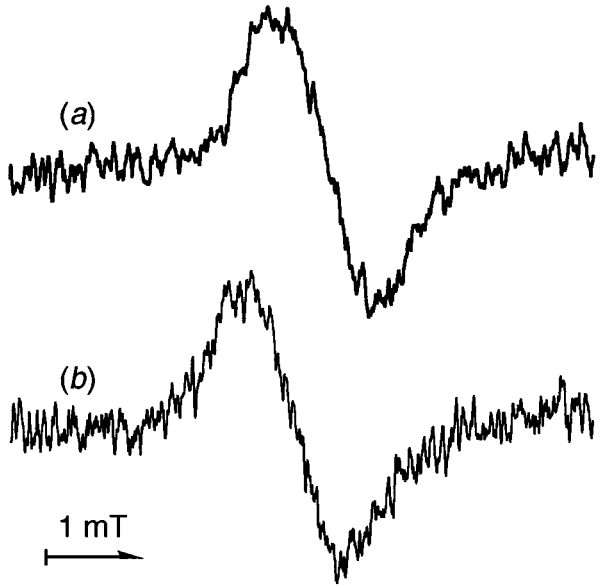

FIGURE 4: EPR spectra of the radical intermediate of (a) QH-AmDH and (b) MADH from *P. denitrificans*, generated by partial reduction with $Na_2S_2O_4$ in pH 7.0 phosphate buffer at room temperature.

well-recognized isosbestic points during the substrate titration.

QH-AmDH gave a strong EPR spectrum on partial reduction with sodium dithionite at pH 7.0, as shown in Figure 4. The total line width of the EPR spectrum was ca. 4.5 mT, which is close to that observed for TTQ-containing MADH (3.8 mT). This is a clear evidence of the presence of the quinonoid cofactor. Similar EPR spectrum was also observed by partial reduction with *n*-butylamine. However, these radical signals disappeared when QH-AmDH was reduced with excess amounts of substrate amine or dithionite.

QH-AmDH exhibited a broad peak centered at 665 nm on the addition of *p*-nitrophenylhydrazine, as shown in Figure 5A. During the spectral change, the heme *c*-related bands remained practically unchanged. This new peak is reasonably ascribed to the formation of *p*-nitrophenylhydrazone adducts of the quinonoid cofactor in QH-AmDH. Figure 5B shows the spectral titration at 665 nm with *p*-nitrophenylhydrazine. The reaction was completed within a few minutes after each addition of *p*-nitrophenylhydrazine. A break point appeared at a 0.91 mol equiv of *p*-nitrophenylhydrazine versus QH-AmDH. The absorption coefficient of the adduct was evaluated as 16.2 mM^{-1} cm^{-1} at 665 nm from the difference spectra. Similar result was obtained using phenylhydrazine in place of *p*-nitrophenylhydrazine, while the shoulder was centered at 615 nm. Then it can be concluded that QH-AmDH has 1 mol of quinonoid cofactor per enzyme in the α subunit.

Electrochemistry and Redox Potential of the Heme c Moiety in QH-AmDH. Direct electrode reaction of QH-AmDH was undetectable at bare glassy carbon or thiol-modified gold electrodes. We further attempted to use the continuous-flow column electrolytic method coupled with photodiode array, since the method provides increased efficiency of electrolysis and improved electrode process (*31*−*33*). Although QH-AmDH was reduced at sufficiently negative potentials (ca. −1.0 V) at a carbon fiber-packed column electrode, the absorption-potential relationship showed irreversible electrochemical process. This might suggest that

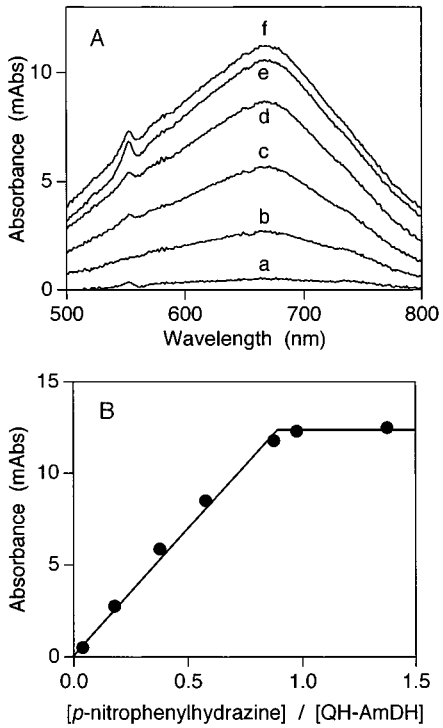

FIGURE 5: (A) Difference absorption spectra of QH-AmDH (2.51 nmol in 3.0 mL) on the addition of *p*-nitrophenylhydrazine at pH 7.0 under aerobic conditions. The amounts of *p*-nitrophenylhydrazine added were (a) 0.10, (b) 0.45, (c) 0.95, (d) 1.45, (e) 2.45, and (f) 3.45 nmol. (B) Spectral titration curve with *p*-nitrophenylhydrazine at 665 nm.

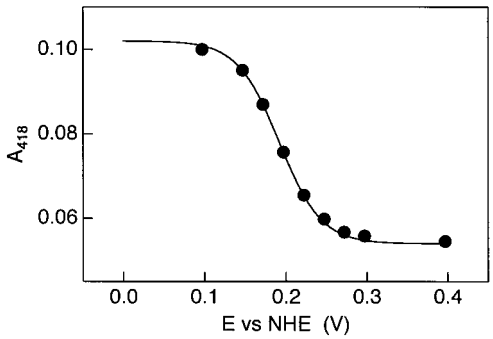

FIGURE 6: Electrochemical titration curve of QH-AmDH taken by a DMBQ (1 mM)-assisted continuous-flow column electrolytic spectroelectrochemical technique at pH 7.0. (●) Experimental data; (—) the fitting curve based on eq 2.

the prosthetic groups are buried in the inside of the enzyme. Therefore, we applied the mediator-assisted continuous-flow column electrolytic spectroelectrochemical technique (*19*) to determine the redox potential of the enzyme.

QH-AmDH exhibited reproducible spectral changes depending on the electrode potential (*E*) in the electrochemically regulated redox buffer containing 1 mM DMBQ at pH 7.0 (0.1 M potassium phosphate, ionic strength 0.3 M with KCl). The spectral changes observed during the potential change were almost identical with those in Figure 3. Any direct information concerning the redox reaction of the quinonoid cofactor was not obtained.

Figure 6 shows the *E* dependence of A_{418} of the background-corrected spectra of QH-AmDH. The electrochemical titration curve was independent of the direction and the width of the potential step, and the flow rate at least up to 1.0 mL

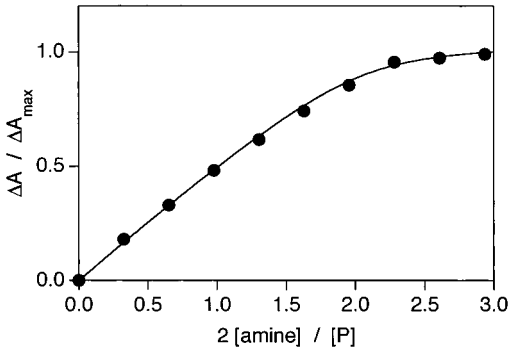

FIGURE 7: Normalized substrate titration curve observed at 418 nm. ΔA and ΔA_{max} are the absorbance change at a given amount and excess amount of *n*-butylamine, respectively; [amine] and [P] are the concentrations of *n*-butylamine (as a 2-electron donor) and QH-AmDH, respectively. The original data were taken from Figure 4. (●) Experimental data; (—) the fitting curve based on eqs 5 and 6.

min^{-1}. These results strongly support that the redox reaction between QH-AmDH and DMBQ reaches equilibrium states under the present conditions. The Nernst equation of the heme *c* redox is given by

$$\frac{[H_{ox}]}{[H_{red}]} = \exp\left[\frac{F}{RT}(E - E_H^{\circ\prime})\right] \equiv \eta_H \quad (1)$$

where $[H_{ox}]$ and $[H_{red}]$ are the concentrations of the heme *c* oxidized and reduced forms of QH-AmDH, respectively; $E_H^{\circ\prime}$ is the redox potential of the heme *c* moiety of QH-AmDH; and *F*, *R*, and *T* have the usual meaning. The relationship between the absorbance (*A*) and *E* can be expressed by

$$A = (\epsilon_{ox}[H_{ox}] + \epsilon_{red}[H_{red}])l = \frac{\epsilon_{ox}\eta_H + \epsilon_{red}}{\eta_H + 1}[P]l \quad (2)$$

where ϵ_{ox} and ϵ_{red} are the absorption coefficients of the oxidized and reduced forms in the heme *c* moiety, respectively, [P] (=$[H_{ox}] + [H_{red}]$) denotes the total concentration of QH-AmDH, and *l* is the light path length. Considering that the plateaus of the electrochemical titration curve in Figure 6 represent the parameters $\epsilon_{ox}[P]l$ and $\epsilon_{red}[P]l$, eq 2 was fitted to the electrochemical titration data with $E_H^{\circ\prime}$ as a adjustable parameter. The Nernstian analysis yielded a well-reproducible curve, as shown by the solid line in Figure 6. $E_H^{\circ\prime}$ was evaluated to be 0.192 V (±0.002 V as the goodness of the fitting).

Electrochemical Analysis of Substrate Titration Curve. Figure 7 represents the normalized substrate titration curve, constructed from the spectral data given in Figure 3. Although the titration data showed curved characteristics, ca. 2 mol equiv of electrons were required for almost complete reduction of the heme *c* moiety in QH-AmDH (note here that *n*-butylamine is a 2-electron donor). Similar characteristic curves were obtained by the ditionite titration. These results seem to support that the substrate titration allows QH-AmDH to reach the redox equilibrium during the titration. The characteristic substrate titration curve was theoretically analyzed in view of spectroelectrochemistry. The ditionite titration curves were not reproducible most probably due to the oxidation of dithionite with trace amounts of dissolved dioxygen.

The quinonoid cofactor will undergo a two-step, 1-electron transfer via the semiquinone state. The reversible redox reaction of the quinonoid cofactor can be expressed as follows:

$$\frac{[Q_{ox}]}{[Q_{sen}]} = \exp\left[\frac{F}{RT}(E - E_{Q1}^{\circ\prime})\right] \equiv \eta_{Q1} \quad (3)$$

$$\frac{[Q_{sen}]}{[Q_{red}]} = \exp\left[\frac{F}{RT}(E - E_{Q2}^{\circ\prime})\right] \equiv \eta_{Q2} \quad (4)$$

where $[Q_{ox}]$, $[Q_{sem}]$, and $[Q_{red}]$ are the concentrations of the oxidized, semiquinone, and reduced forms in the quinonoid moiety of QH-AmDH, respectively, and $[Q_{ox}] + [Q_{sem}] + [Q_{red}] = [P]$; $E_{Q1}^{\circ\prime}$ and $E_{Q2}^{\circ\prime}$ are the redox potentials of the quinone/semiquinone and semiquinone/quinol redox couples of QH-AmDH, respectively. Since the spectral change during the substrate titration is ascribed to the redox reaction of the heme *c* moiety alone, the relative spectral change ($\Delta A/\Delta A_{max}$) depicted in Figure 7 can be expressed by

$$\frac{\Delta A}{\Delta A_{max}} = \frac{[H_{red}]}{[P]} = \frac{1}{\eta_H + 1} \quad (5)$$

On the other hand, the bimolecular rate constant between QH-AmDH and *n*-butylamine [k_{cat}/K_m(S)] is sufficiently large (Table 1) and each of the spectra was recorded sufficiently after the addition of *n*-butylamine to reach time-independent state. This means that *n*-butylamine is almost completely oxidized up to the stoichiometric amount and that the enzyme is in redox equilibrium. Therefore, the relative amount of the substrate against the total enzyme (2[amine]/[P]) is equivalent to the reduced equivalent of QH-AmDH and is expressed by

$$\frac{2[amine]}{[P]} = \frac{[Q_{sen}] + 2[Q_{red}] + [H_{red}]}{[P]} = \frac{\eta_{Q2} + 2}{\eta_{Q2}\eta_{Q1} + \eta_{Q2} + 1} + \frac{1}{\eta_H + 1} \quad (6)$$

Equation 6 indicates that the equilibrated redox potential of the enzyme solution *E* is determined by 2[amine]/[P] for given values of $E_{Q1}^{\circ\prime}$, $E_{Q2}^{\circ\prime}$, and $E_H^{\circ\prime}$. The $\Delta A/\Delta A_{max}$ value is in turn calculated from *E* and $E_H^{\circ\prime}$ according to eq 5. This means that $\Delta A/\Delta A_{max}$ and 2[amine]/[P] values are related to each other using *E* as a medium variable. Thus, the nonlinear least-squares analysis of $\Delta A/\Delta A_{max}$ vs 2[amine]/[P] curve allows evaluation of two parameters among $E_{Q1}^{\circ\prime}$, $E_{Q2}^{\circ\prime}$, and $E_H^{\circ\prime}$ (or evaluation of the difference of the redox potentials such as $E_{Q1}^{\circ\prime} - E_H^{\circ\prime}$ and $E_{Q2}^{\circ\prime} - E_H^{\circ\prime}$).

The titration curve in Figure 7 was successfully reproduced on the basis of eqs 5 and 6 using $E_{Q1}^{\circ\prime}$ and $E_{Q2}^{\circ\prime}$ as adjustable parameters, the $E_H^{\circ\prime}$ value evaluated in the above section being used as a fixed parameter. The values of $E_{Q1}^{\circ\prime}$ and $E_{Q2}^{\circ\prime}$ for the best fit were 0.19 and 0.11 V, respectively, with a standard deviation of 0.003 and 0.01 V, respectively, as the goodness of the fitting. The situation that $E_H^{\circ\prime} \approx E_{Q1}^{\circ\prime} > E_{Q2}^{\circ\prime}$ means that the reduction of the heme *c* undergoes almost simultaneously with the reduction of the quinonoid cofactor to the semiquinone state, resulting in the almost 2 mol equiv characteristics (Figure 7). The semiquinone is then fully

reduced to the quinol form, probably by the intermolecular electron transfer between the partially reduced QH-AmDH.

DISCUSSION

This study revealed the expression of at least two amine dehydrogenases, QH-AmDH and MADH, in *P. denitrificans* grown with methylamine as a sole source of carbon and energy. The use of *n*-butylamine or benzylamine in place of methylamine enhances the expression of QH-AmDH and suppresses the MADH expression almost completely. QH-AmDH has a large K_m(S) for methylamine (Table 1) compared with MADH [K_m(S) = 20 μM (*29*)] and has relatively broad substrate specificity for primary amines. Therefore, it would be expected that QH-AmDH plays a significant role at increased concentrations of methylamine or for various kinds of primary amines other than methylamine. Furthermore, QH-AmDH seems to be essential for *P. denitrificans* in efficient utilization and/or detoxification of amines.

QH-AmDH isolated from *P. denitrificans* IFO 12442 is the second example as a quinohemoprotein amine dehydrogenase; the first one is AMDH from *P. putida*. Although some properties of QH-AmDH are similar to those of AMDH from *P. putida*, the enzyme structure is significantly different from each other. QH-AmDH from *P. denitrificans* has an $\alpha\beta$ subunit structure and the α subunit contains one quinonoid cofactor and one heme *c*. In contrast, AMDH from *P. putida* has a heterotrimer structure and the largest and smallest subunits contain two heme *c* moieties and (one) quinonoid cofactor, respectively (*18*). The substrate specificity of QH-AmDH is also different from that of AMDH. Methylamine can serve as a suitable substrate of QH-AmDH at least at relatively high concentrations [due to large K_m-(S), see Table 1], while AMDH can hardly work on methylamine (*15*, *17*).

The α subunit in QH-AmDH exhibits the positive response in the quinone-dependent redox-cycling stain even after denaturation in SDS−PAGE. Therefore, the quinonoid cofactor can be considered to form a covalent bond with the peptide chain of the α subunit, and then pyrroloquinoline quinone (PQQ) may be ruled out as the quinonoid cofactor of QH-AmDH. This consideration is also supported by the EDTA-insensitive property of the QH-AmDH activity, since PQQ enzymes frequently require some alkali earth metal ion removable with EDTA.

Practically all of the absorption spectral change during the redox reaction of QH-AmDH is assigned to the heme *c* alone. This suggests that the absorption coefficient of the quinonoid cofactor is much smaller than that of heme *c*, probably $\epsilon <$ 10 mM^{-1} cm^{-1} around 400 nm and $\epsilon < 1$ mM^{-1} cm^{-1} around 500 nm. The oxidized and reduced forms of the TTQ-containing MADH have absorption coefficients as $\epsilon = 26.2/2$ mM^{-1} cm^{-1} (per monomer) at 440 nm and $\epsilon = 56.4/2$ mM^{-1} cm^{-1} at 330 nm, respectively (*34*). A TTQ model compound have also similar absorption coefficients [$\epsilon = 9.2$ mM cm^{-1} at 434 nm for the oxidized form and $\epsilon = 12.3$ mM cm^{-1} at 306 nm for the reduced form (*11*)]. Therefore, TTQ might be ruled out as the quinonoid cofactor of QH-AmDH; if TTQ were the cofactor of QH-AmDH, any spectral change due to the redox of the quinonoid cofactor could be observed. Such characteristics of QH-AmDH as small absorption coefficients of the quinonoid cofactor might resemble topaquinone-containing amine oxidase [$\epsilon = 2.0-5.7$ mM^{-1} cm^{-1} at 460−500 nm for the oxidized form (*35*)], but there is no report on topaquinone-containing amine "dehydrogenase".

The spectral properties of the *p*-nitrophenylhydrazone and/or phenylhydrazone adducts of QH-AmDH are quite different from those derived from the other known quinonoid cofactors. The *p*-nitrophenylhydrazone of PQQ, topaquinone, and TTQ have absorbance maximum around 450 nm at neutral pH (*36*−*38*). The longer wavelength of the absorption maximum of the hydrazone adducts of QH-AmDH (665 and 615 nm for *p*-nitrophenylhydrazone and phenylhydrazone adducts, respectively) might suggest a higher resonance structure of the hydrazone adduct of the quinonoid cofactor in QH-AmDH. However, the relatively small absorption coefficient of the adduct as well as the native quinonoid cofactor seems to suggest some steric hindrance. Anyway, these spectral characteristics might suggest a new quinonoid cofactor.

In this work, the spectroelectrochemical analysis of the electrochemical and substrate titration curves allowed the evaluation of the redox potentials of the heme *c* and the quinonoid cofactor ($E^{\circ}_{H}{}' = 0.192$ V, $E^{\circ}_{Q1}{}' = 0.19$ V, and $E^{\circ}_{Q2}{}' = 0.11$ V). The overall two-electron redox potential of the quinonoid cofactor [$=(E^{\circ}_{Q1}{}' + E^{\circ}_{Q2}{}')/2 = 0.15$ V] is close to the redox potential of TTQ in MADH (0.10 V) (*34*, *39*). The semiquinone formation constant (K_{sem}) defined by eq 7 is calculated to be 23.

$$K_{sen} = \frac{[Q_{sen}]^2}{[Q_{ox}][Q_{red}]} = \exp\left[\frac{F}{RT}(E^{\circ}_{Q1}{}' - E^{\circ}_{Q2}{}')\right] \qquad (7)$$

Such stabilization of the semiquinone is in accord with the strong intensity of the EPR spectrum and might suggest that the quinonoid cofactor exists in hydrophobic circumstances of QH-AmDH.

Judging from the redox potentials evaluated here, it can be concluded that an intramolecular electron transfer occurs from the quinonoid cofactor to the heme *c* moiety in QH-AmDH, where the quinonoid cofactor works as a 2-electron acceptor for the substrate and as a 1-electron donor for the heme *c* moiety. The physiological electron acceptors for quinoprotein amine dehydrogenases have been proposed to be type I blue copper proteins: amicyanin for MADH (*40*) and azurin for AADH (*41*). As studied extensively by Davidson's group, the electron passed to amicyanin from MADH is transferred to the terminal oxidase via cytochrome c_{551i} (*40*, *42*, *43*). Because $E^{\circ}_{H}{}'$ of the heme *c* in QH-AmDH is very close to the reported value for cytochrome c_{551i} (0.19 V) (*44*), it might be expected that the heme *c* in the QH-AmDH is linked to the terminal oxidase. Further kinetic and thermodynamic study of QH-AmDH and the identification of the quinonoid cofactor are in progress.

ACKNOWLEDGMENT

The authors wish to thank Professor Osao Adachi, Department of Biological Chemistry, Yamaguchi University, Japan, for his kind advice in isolation of MADH. The authors also thank Mr. Kazumichi Iwasa for his experimental assistance.

REFERENCES

1. Eady, R. R., and Large, P. J. (1968) *Biochem. J. 106*, 245−255.
2. Mehta, R. J. (1977) *Can. J. Microbiol. 23*, 402−406.
3. Matsumoto, T. (1978) *Biochim. Biophys. Acta 522*, 291−302.
4. Kenney, W. C., and McIntire, W. (1983) *Biochemistry 22*, 3858−3868.
5. Vellieux, F. M. D., Frank, J. Jzn., Swarte, M. B. A., Groendijk, H., Duine, J. A., Drenth, J., and Hol, W. G. J. (1986) *Eur. J. Biochem. 154*, 383−386.
6. Husain, M., and Davidson, V. L. (1987) *J. Bacteriol. 169*, 1712−1717.
7. Iwaki, M., Yagi, T., Horiike, K., Saeki, Y., Ushijima, T., and Nozaki, M. (1983) *Arch. Biochem. Biophys. 220*, 253−262.
8. Govindaraj, S., Eisenstein, E., Jones, L. H., Sanders-Leohr, J., Chistoserdov, A. Y., Davidson, V. L., and Edwards, S. L. (1994) *J. Bacteriol. 176*, 2922−2929.
9. McIntire, W. S., Wemmer, D. E., Chistoserdov, A., and Lidstrom, M. E. (1991) *Science 252*, 817−824.
10. Itoh, S., Ogino, M., Komatsu, M., and Ohshiro, Y. (1992) *J. Am. Chem. Soc. 114*, 7294−7295.
11. Itoh, S., Ogino, M., Haranou, S., Terasaki, T., Ando, T., Komatsu, M., Ohshiro, Y., Fukuzumi, S., Kano, K., Takagi, K., and Ikeda, T. (1995) *J. Am. Chem. Soc. 117*, 1485−1493.
12. Itoh, S., Takada, N., Haranou, S., Ando, T., Komatsu, M., Ohshiro, Y., and Fukuzumi, S. (1996) *J. Org. Chem. 61*, 8967−8974.
13. Itoh, S., Takada, N., Ando, T., Haranou, S., Huang, X., Uenoyama, Y., Ohshiro, Y., Komatsu, M., and Fukuzumi, S. (1997) *J. Org. Chem. 62*, 5898−5907.
14. Kano, K., Nakagawa, M., Takagi, K., and Ikeda, T. (1997) *J. Chem. Soc., Perkin Trans. 2 1997*, 1111−1119.
15. Durham, D. R., and Perry, J. J. (1978) *J. Bacteriol. 134*, 837−843.
16. Durham, D. R., and Perry, J. J. (1978) *J. Bacteriol. 135*, 981−986.
17. Shinagawa, E., Matsushita, K., Nakashima, K., Adachi, O., and Ameyama, M. (1988) *Agric. Biol. Chem. 52*, 2255−2263.
18. Adachi, O., Kubota, T., Hacisalihoglu, A., Toyama, H., Shinagawa, E., Duine, J. A., and Matsushita, K. (1998) *Biosci. Biotechnol. Biochem. 62*, 469−478.
19. Torimura, M., Mochizuki, M., Kano, K., Ikeda, T., and Ueda, T. (1998) *Anal. Chem. 70*, 4690−4695
20. Alefounder, P. R., and Ferguson, S., J. (1981) *Biochem. Biophys. Res. Commun. 98*, 778−784
21. Davidson, V. L. (1990) *Methods Enzymol. 188*, 241−246
22. Davis, B. J. (1964) *Ann. N. Y. Acad. Sci. 121*, 404−427.
23. Laemmli, U. K. (1970) *Nature 227*, 680−685.
24. Paz, M. A., Flückiger, R., Boak, A., Kagen, H. M., and Gallop, P. M. (1991) *J. Biol. Chem. 266*, 689−692.
25. Thomas, P. E., Ryan, D., and Levin, W. (1976) *Anal. Biochem. 75*, 168−176.
26. Berry, E. A., and Trumpower, B. L. (1987) *Anal. Biochem. 161*, 1−15.
27. Markwell, M. A. K., Haas, S. M., Bieber, L. L., and Tolbert, N. E. (1978) *Anal. Biochem. 87*, 206−210.
28. Davidson, V. L. (1993) in *Principal and Application of Quinoproteins* (Davidson, V. L., Ed.) pp 73−95, Marcel Deckker, New York.
29. Davidson, V. L. (1989) *Biochem. J. 261*, 107−111.
30. Kasprzak, A. J., and Steenkamp, D. J. (1983) *J. Bacteriol. 156*, 349−353.
31. Oyama, M., Okada, M., and Okazaki, S. (1993) in *Redox Mechanisms and Interfacial Properties of Molecules of Biological Importance* (Schultz, F. A., and Taniguchi, I., Eds.) pp 343−354, The Electrochemical Soc., Pennington, NJ.
32. Torimura, M., Kano, K., Ikeda, T., and Ueda, T. (1997) *Chem. Lett. 1997*, 525−526.
33. Torimura, M., Mochizuki, M., Kano, K., Ikeda, T., and Ueda, T. (1998) *J. Electroanal. Chem. 451*, 229−235.
34. Husain, M., Davidson, V. L., Gray, K. A., and Knaff, D. B. (1987) *Biochemistry 26*, 4139−4142.
35. McIntire, W. S., and Hartmann, C. (1993) in *Principal and Application of Quinoproteins* (Davidson, V. L., Ed.) pp 97−171, Marcel Deckker, New York.
36. Palcic, M. M., and Janes, S. M. (1995) *Methods Enzymol. 258*, 34−38.
37. Janes, S. M., Palcic, M. M., Scaman, C. H., Smith, A. J., Brown, D. E., Dooley, D. M., Mure, M., and Klinman, J. P. (1992) *Biochemistry 31*, 12147−12154.
38. Kenney, W. C., and McIntire, W. (1983) *Biochemistry 22*, 3858−3868.
39. Burrows, A. L., Hill, H. A. O., Leese, T. A., McIntire, W. S., Nakayama, H., and Sanghera, G. S. (1991) *Eur. J. Biochem. 199*, 73−78.
40. Husain, M., and Davidson, V. L. (1985) *J. Biol. Chem. 260*, 14626−14629.
41. Edwards, S. L., Davidson, V. L., Hyun, Y.-L., and Wingfield, P. T. (1995) *J. Biol. Chem. 270*, 4293−4298.
42. Husain, M., and Davidson, V. L. (1986) *J. Biol. Chem. 261*, 8577−8580.
43. Chen, L., Durley, R. C. E., Mathews, F. S., and Davidson, V. L. (1994) *Science 264*, 86−90.
44. Gray, K. A., Knaff, D. B., Husain, M., and Davidson, V. L. (1986) *FEBS Lett. 207*, 239−242.

BI9828268